

Scalar/Dirac perturbations of the Reissner-Nordström black hole and Painlevé transcendents

João Paulo Cavalcante,^{1,*} and Bruno Carneiro da Cunha^{1,†}

¹*Departamento de Física, Universidade Federal de Pernambuco, 50670-901, Recife, Brazil*

We investigate spin-0 and spin- $\frac{1}{2}$ perturbations for non-extremal and extremal Reissner-Nordström backgrounds using the isomonodromic method. We calculate the fundamental quasinormal modes (QNMs) associated with each perturbation as a function of the electromagnetic coupling qQ and ratio Q/M . After corroborating the literature values for generic qQ and Q/M , we turn to study the near-extremal limit. In parallel with the study of QNMs for the Kerr geometry, we find the existence of “non-damping” modes for qQ above a spin-dependent critical value, and locate the bifurcation point in the $q - Q$ parameter space.

I. INTRODUCTION

The Reissner-Nordström (RN) metric is a solution to the Einstein-Maxwell field equations, corresponding to a non-rotating charged black hole of mass M and charge Q . In static and spherically symmetric coordinates, the metric is given by [1]

$$ds^2 = -\frac{\Delta}{r^2} dt^2 + \frac{r^2}{\Delta} dr^2 + r^2(d\theta^2 + \sin^2\theta d\phi^2), \quad \Delta = r^2 - 2Mr + Q^2 = (r - r_+)(r - r_-), \quad (1)$$

and in the Coulomb gauge the only non-vanishing component of the electromagnetic potential A_μ is $A_0 = -\frac{Q}{r}$. The roots of Δ will be called r_+ and r_- . For $Q < M$, we have the non-extremal RN black hole and r_+ and r_- are the event and Cauchy horizons of the black hole, respectively, with $r_+ > r_-$. When $Q = M$, the black hole is extremal, where the roots are equal, $r_+ = r_-$. In turn, for $Q > M$, the black hole space-time has a naked singularity, with Δ having no real root.

Linear perturbations of massless charged scalar ($s = 0$) and spinor ($s = \frac{1}{2}$) fields in the RN background can be effectively unified in an equation similar to the radial Teukolsky master equation (TME) for the Kerr black hole [2]. The master equation can be derived by separating the Klein-Gordon and the Dirac equations in the RN background [3], arriving at

$$\Delta^{-s} \frac{d}{dr} \left(\Delta^{1+s} \frac{dR_s(r)}{dr} \right) + \left(\frac{K(r)^2 - 2is(r-M)K(r)}{\Delta} + 4is\omega r - 2isqQ - {}_s\lambda_\ell \right) R_s(r) = 0 \quad (2)$$

where, $s = 0, \pm 1/2$, $K(r) = \omega r^2 - qQr$ and ${}_s\lambda_\ell = (\ell - s)(\ell + s + 1)$ is the separation constant. The angular dependence of the solutions is given by the usual spin-weighted spherical harmonics $Y_{\ell m}^s(\theta, \phi)$, where the parameters ℓ and m satisfy the usual constraints: ℓ is a non-negative integer and a non-negative half-integer for bosonic and fermionic case, respectively, with $\ell \geq |s|$. For m , one has essentially $-\ell \leq m \leq \ell$ [4, 5].

Quasinormal modes (QNMs) are in general an useful tool to understand physical properties of black hole backgrounds, such as linear stability. For the RN black hole, QNMs are solutions of (2) that correspond to purely outgoing waves at the outer horizon and purely ingoing at infinity. The spectrum of these boundary conditions is discrete, with complex frequencies, the real part representing the oscillation character of the perturbations and the imaginary part the damping factor. The frequencies are not only functions of the mass M and charge Q of the black hole, but also of the charge q and spin s of the perturbing field. The spectrum is labelled by integers m , ℓ and n with usual interpretations.

The study of electromagnetic and gravitational QNMs in RN space-time was considered in [6], using a semiclassical (WKB) approach. In [7], Leaver considered the same problem using the solution of the 3-term recurrence equation using continued fraction (CF) method that he introduced in [8]. The CF method allowed for improved accuracy when compared with the WKB approximation, but the numerics suffered for the near-extremal case $Q \rightarrow M$. The continued fraction method was later improved by [9], and used to study the extremal case, obtaining values for the massless scalar ($s = 0$), electromagnetic and gravitational cases when $Q = M$.

* joapaulocavalcante@hotmail.com.br

† bruno.cunha@ufpe.br

For spinorial ($s = 1/2$) perturbations, the initial analysis was made in [10], approximating the interaction between the field and the black hole by a Pöschl-Teller potential. In [11], the CF method was applied for the non-extremal RN black hole to obtain the QNMs frequencies for spins 0 and 1/2, and various values of qQ . This analysis was extended for extremal RN black holes in [12], using the same strategy developed in [9]. In these analysis, the study of the extremal limit, where $Q \rightarrow M$ is hindered by numerical accuracy of the CF method, and the behavior the QNMs as one approaches the extremal point is still in need of clarification.

In a series of papers [13, 14], building on previous work [15–17], properties of the scattering of the fields were related to the monodromy properties of the solutions of the confluent Heun differential equation governing the black hole perturbations. In turn, these monodromy properties are obtainable from the parameters of the differential equation by means of the Riemann-Hilbert map, and more conveniently expressed in terms of the Fifth Painlevé transcendent tau function τ_V . By using the general expansion of τ_V given in [18, 19], one achieves an analytical solution to the scattering problem, given implicitly in terms of transcendental equations which can be studied numerically. The relation between these expansions and the properties of conformal blocks both in the $c = 1$ [14] and semiclassical cases [20] hints at a possible underlying connection between black hole physics and conformal field theories. At any rate, the procedural solution of the monodromy problem in terms of conformal blocks provide us with a numerical recipe that is not encumbered by the drawbacks of the CF method. In [21] the τ_V method was used to study the QNMs frequencies for the Kerr black hole, focussing particularly in the extremal limit.

Our main objective in this work is to apply the isomonodromic method to study the QNMs of scalar and spinorial massless perturbations of the RN black hole. We will treat the black hole and field charges, respectively Q and q , generically, but will focus on the extremal limit. The plan of the paper is as follows: in Section II we revise the RH method, and in Section III we derive the relevant parameters for the confluent Heun equation associated to (2) and present the results of the numerical analysis for $Q < M$ and $Q \rightarrow M$ separately. In Section IV we deal with the extremal case separately. We close by commenting the results in Section V and presenting some future prospects. For completeness, we included an Appendix A with the relevant technical details on the tau functions and monodromy properties of the solutions.

II. MONODROMY PROPERTIES

Let us revise the isomonodromic method used in [14, 21]. The radial equation (2) is a particular case of the confluent Heun differential equation

$$\frac{d^2 y}{dz^2} + \left[\frac{1 - \theta_0}{z} + \frac{1 - \theta_0}{z - t_0} \right] \frac{dy}{dz} - \left[\frac{1}{4} + \frac{\theta_\star}{2z} + \frac{t_0 c_{t_0}}{z(z - t_0)} \right] y(z) = 0, \quad (3)$$

defined for complex z , with regular singular behavior at 0 and t_0 and an irregular singularity of Poincaré rank 1 at $z = \infty$.

The Riemann-Hilbert map is defined from the accessory parameter c_{t_0} and conformal modulus t_0 of (3) to the *monodromy data* $\{\sigma, \eta\}$ of its solutions. As shown in [14], the map is implicitly expressed by the following equations

$$\tau_V(\vec{\theta}; \sigma, \eta; t_0) = 0, \quad t_0 \frac{d}{dt} \log \tau_V(\vec{\theta}_-; \sigma - 1, \eta; t_0) - \frac{\theta_0(\theta_t - 1)}{2} = t_0 c_{t_0}, \quad (4)$$

where $\vec{\theta} = \{\theta_0, \theta_t, \theta_\star\}$ are the parameters in (3) associated to the local monodromy of solutions. The first equation is the Painlevé V version of the Toda equation, studied in [22], and was shown in [14] to be related to the well-posedness of the initial value problem for the Painlevé V transcendent equation. The monodromy arguments of the second equation are shifted: $\vec{\theta}_- = \{\theta_0, \theta_t - 1, \theta_\star + 1\}$, and defines the accessory parameter c_{t_0} as the logarithm derivative of the isomonodromic tau function defined by the groundbreaking papers of the Kyoto school [23–25]. We refer to [14] for details on the relation between τ_V , the fifth Painlevé transcendent and the theory of isomonodromic deformations.

The role of the so-called composite monodromy parameters $\{\sigma, \eta\}$ was studied in [19], in the context of confluent conformal blocks. In [26] (see also [21]), it was noted that σ parametrizes the so-called Floquet solutions of (3), and a direct relation between σ and c_{t_0} was derived,

$$t_0 c_{t_0} = \frac{(\sigma - 1)^2 - (\theta_t + \theta_0 - 1)^2}{4} + \frac{\theta_\star(\sigma(\sigma - 2) + \theta_t^2 - \theta_0^2)}{4\sigma(\sigma - 2)} t_0 + \left[\frac{1}{32} + \frac{\theta_\star^2(\theta_t^2 - \theta_0^2)^2}{64} \left(\frac{1}{\sigma^3} - \frac{1}{(\sigma - 2)^3} \right) + \frac{(1 - \theta_\star^2)(\theta_0^2 - \theta_t^2)^2 + 2\theta_\star^2(\theta_0^2 + \theta_t^2)}{32\sigma(\sigma - 2)} - \frac{(1 - \theta_\star^2)((\theta_0 - 1)^2 - \theta_t^2)((\theta_0 + 1)^2 - \theta_t^2)}{32(\sigma + 1)(\sigma - 3)} \right] t_0^2 + \mathcal{O}(t_0^3). \quad (5)$$

This formula can be obtained by various different methods, and the equivalence between the semiclassical confluent conformal blocks approach of [20, 26, 27] and the $c = 1$ isomonodromic approach of [14, 19] is a non-trivial consequence of the exponentiation property of conformal blocks.

The practical use of the Riemann-Hilbert map (4) relies on effective ways to compute τ_V . In a seminal work [28], Jimbo showed that the isomonodromic τ functions can be conveniently expanded in terms of the monodromy parameters $\{\sigma, \eta\}$, and, in [18], the authors used the relation between isomonodromic deformations, conformal blocks and Seiberg-Witten theory to propose the full expansion of τ_V in terms of Nekrasov functions. Later, in [19], the Painlevé V τ function was recast in terms of the Fredholm determinant associated to the actual Riemann-Hilbert problem of finding analytic functions on the complex plane with prescribed jumps. The latter formulation of τ_V is particularly suited for numerical studies, as the authors have conducted for the fundamental QNMs for generic spin perturbations of the Kerr black holes in [21], where the reader can find complete formulas. For our purposes, the small- t expansion of the τ_V will suffice (A1). For σ in the fundamental domain $-1 < \Re(\sigma) < 1$, we have

$$\begin{aligned} \tau_V(\vec{\theta}; \sigma, \eta; t) = C_V(\vec{\theta}; \sigma) t^{\frac{1}{4}(\sigma^2 - \theta_0^2 - \theta_t^2)} e^{\frac{1}{2}\theta_t t} & \left(1 - \left(\frac{\theta_t}{2} - \frac{\theta_*}{4} + \frac{\theta_*(\theta_0^2 - \theta_t^2)}{4\sigma^2} \right) t \right. \\ & \left. - \frac{(\theta_* + \sigma)((\sigma + \theta_t)^2 - \theta_0^2)}{8\sigma^2(\sigma - 1)^2} \kappa_V^{-1} t^{1-\sigma} - \frac{(\theta_* - \sigma)((\sigma - \theta_t)^2 - \theta_0^2)}{8\sigma^2(\sigma + 1)^2} \kappa_V t^{1+\sigma} + \mathcal{O}(t^2, |t|^{2\pm 2\Re\sigma}) \right), \end{aligned} \quad (6)$$

where C_V is an arbitrary (non-zero) constant and

$$\kappa_V = e^{i\pi\eta} \Pi_V = e^{i\pi\eta} \frac{\Gamma(1 - \sigma)^2 \Gamma(1 + \frac{1}{2}(\theta_* + \sigma)) \Gamma(1 + \frac{1}{2}(\theta_t + \theta_0 + \sigma)) \Gamma(1 + \frac{1}{2}(\theta_t - \theta_0 + \sigma))}{\Gamma(1 + \sigma)^2 \Gamma(1 + \frac{1}{2}(\theta_* - \sigma)) \Gamma(1 + \frac{1}{2}(\theta_t + \theta_0 - \sigma)) \Gamma(1 + \frac{1}{2}(\theta_t - \theta_0 - \sigma))}. \quad (7)$$

In general, scattering amplitudes can be written in terms of the monodromy parameters [13, 14], so by solving the Riemann-Hilbert map one can solve the scattering problem. For the calculation of quasinormal modes, we must impose boundary conditions such that there is no energy flux out of the black hole event horizon at r_+ and no energy flux out at infinity. In [21], the authors showed that these boundary conditions can be cast in terms of monodromy data as

$$e^{i\pi\eta} = e^{-i\pi\sigma} \frac{\sin \frac{\pi}{2}(\theta_* + \sigma) \sin \frac{\pi}{2}(\theta_t + \theta_0 + \sigma) \sin \frac{\pi}{2}(\theta_t - \theta_0 + \sigma)}{\sin \frac{\pi}{2}(\theta_* - \sigma) \sin \frac{\pi}{2}(\theta_t + \theta_0 - \sigma) \sin \frac{\pi}{2}(\theta_t - \theta_0 - \sigma)}. \quad (8)$$

This condition is equivalent to imposing that the connection matrix C_t between local solutions of (3) constructed around the $z = t_0$ and local solutions at $z = \infty$ is lower triangular, see part A 1 of the Appendix.

With the explicit formulation of τ_V , the Riemann-Hilbert map (4) can in principle be used to compute the monodromy parameters $\{\sigma, \eta\}$ given the parameters of the confluent Heun equation (3). Given generic parameters, the QNM condition (8) overdetermines the system and thus will allow for solutions only for a discrete set of values of t_0 and c_{t_0} . Operationally speaking, one can use the expansion of τ_V (6) to solve the first equation in (4) to compute η in terms of σ , t_0 and the $\vec{\theta}$, and the expansion of the accessory parameter (5) to compute σ in terms of the parameters of (3).

Following this strategy, one notes from (6) that τ_V is meromorphic in $\kappa_V t^\sigma$ so the equation $\tau_V(\vec{\theta}, \sigma, \eta, t_0) = 0$ can be inverted to define a series for $\kappa_V t^\sigma$, or $e^{i\pi\eta}$ in terms of t_0 . Assuming that σ satisfies $0 < \Re(\sigma) < 1$, we arrive at the expression

$$\Theta_V(\vec{\theta}; \sigma) e^{i\pi\eta} t_0^{\sigma-1} = \chi_V(\vec{\theta}; \sigma; t_0), \quad (9)$$

with $\Theta_V(\vec{\theta}; \sigma)$ expressed in terms of ratios of gamma functions

$$\Theta_V(\vec{\theta}; \tilde{\sigma}) = \frac{\Gamma^2(2 - \sigma)}{\Gamma^2(\sigma)} \frac{\Gamma(\frac{1}{2}(\theta_* + \sigma))}{\Gamma(1 + \frac{1}{2}(\theta_* - \sigma))} \frac{\Gamma(\frac{1}{2}(\theta_t + \theta_0 + \sigma))}{\Gamma(1 + \frac{1}{2}(\theta_t + \theta_0 - \sigma))} \frac{\Gamma(\frac{1}{2}(\theta_t - \theta_0 + \sigma))}{\Gamma(1 + \frac{1}{2}(\theta_t - \theta_0 - \sigma))} \quad (10)$$

and the function $\chi_V(\vec{\theta}; \sigma; t_0)$ analytic for t_0 small, with expansion

$$\begin{aligned} \chi_V(\vec{\theta}; \tilde{\sigma}; t_0) = 1 + (\tilde{\sigma} - 1) \frac{\theta_*(\theta_t^2 - \theta_0^2)}{\tilde{\sigma}^2(\tilde{\sigma} - 2)^2} t_0 + & \left[\frac{\theta_*^2(\theta_t^2 - \theta_0^2)^2}{64} \left(\frac{5}{\tilde{\sigma}^4} - \frac{1}{(\tilde{\sigma} - 2)^4} - \frac{2}{(\tilde{\sigma} - 2)^2} + \frac{2}{\tilde{\sigma}(\tilde{\sigma} - 2)} \right) \right. \\ & - \frac{(\theta_t^2 - \theta_0^2)^2 + 2\theta_*^2(\theta_t^2 + \theta_0^2)}{64} \left(\frac{1}{\tilde{\sigma}^2} - \frac{1}{(\tilde{\sigma} - 2)^2} \right) \\ & \left. + \frac{(1 - \theta_*^2)(\theta_t^2 - (\theta_0 - 1)^2)(\theta_t^2 - (\theta_0 + 1)^2)}{128} \left(\frac{1}{(\tilde{\sigma} + 1)^2} - \frac{1}{(\tilde{\sigma} - 3)^2} \right) \right] t_0^2 + \mathcal{O}(t_0^3). \end{aligned} \quad (11)$$

For $\Re(\sigma) < 0$, we also have an expression similar for (9), where one simply changes to $\sigma \rightarrow -\sigma$ and $e^{i\pi\eta} \rightarrow e^{-i\pi\eta}$. Although it will not be necessary for our purposes, one can in principle compute the expansion of χ_V to arbitrary order in t_0 .

Finally, we can incorporate the condition (8) into the expression (9). Using the definition of Θ_V , and the identity $\Gamma(z)\Gamma(1-z) = \pi/\sin(\pi z)$, one obtains, when η satisfies (8),

$$\Theta_V(\vec{\theta}, \sigma) e^{i\pi\eta} = -e^{-i\pi\sigma} \Theta_V(-\vec{\theta}, \sigma), \quad (12)$$

Substituting back into (9), we find

$$-e^{-i\pi\sigma} \Theta_V(-\vec{\theta}, \sigma) t_0^{\sigma-1} = \chi_V(\vec{\theta}; \sigma; t_0), \quad (13)$$

again assuming $\Re(\sigma) > 0$. For $\Re(\sigma) < 0$, one finds the right expansion by simply sending $\sigma \rightarrow -\sigma$ in (13). With the expression (13), one can then consider for the QNM problem the overdetermined system of equations consisted by (5) and (13), with σ the free parameter.

III. RADIAL SYSTEM AND NUMERICAL RESULTS FOR $0 \leq Q \leq M$

After these generic comments, let us consider the RH map (4) for the radial equation (2). The radial equation (2) can be brought to the standard form (3) by the change of variables

$$R(r) = (r - r_-)^{-(s+\theta_-)/2} (r - r_+)^{-(s+\theta_+)/2} y(z), \quad z = 2i\omega(r - r_-) \quad (14)$$

where

$$\begin{aligned} \theta_- = s + \frac{i}{2\pi T_-} \left(\omega - \frac{qQ}{r_-} \right), \quad \theta_+ = s + \frac{i}{2\pi T_+} \left(\omega - \frac{qQ}{r_+} \right), \quad \theta_* = -2s + 2i(2M\omega - qQ), \\ 2\pi T_{\pm} = \frac{r_{\pm} - r_{\mp}}{2r_{\pm}^2}, \quad r_{\pm} = M \pm \sqrt{M^2 - Q^2}, \end{aligned} \quad (15)$$

one can find the accessory parameter and the modulus

$$z_0 c_{z_0} = {}_s\lambda_{l,m} + 2s - i(1-2s)qQ + (2qQ + i(1-3s))\omega r_+ + i(1-s)\omega r_- - 2\omega^2 r_+^2, \quad z_0 = 2i\omega(r_+ - r_-). \quad (16)$$

In the following it will be convenient to parametrize $Q/M = \cos \nu$ with $\nu \in [0, \pi/2]$, with the extremal limit $r_- \rightarrow r_+$ corresponding to $\nu \rightarrow 0$. In terms of ν , the monodromy parameters (15) are rewritten as

$$\begin{aligned} \theta_- = -s - \frac{i}{2\pi T_-} \left(\omega - \frac{qQ}{M(1 - \sin \nu)} \right), \quad \theta_+ = s + \frac{i}{2\pi T_+} \left(\omega - \frac{qQ}{M(1 + \sin \nu)} \right), \quad \theta_* = -2s + 2i(2M\omega - qQ) \\ 2\pi T_{\pm} = \pm \frac{\sin \nu}{M(1 \pm \sin \nu)^2}, \quad r_{\pm} = M(1 \pm \sin \nu), \end{aligned} \quad (17)$$

and the accessory parameters(16)

$$\begin{aligned} z_0 c_{z_0} = {}_s\lambda_{l,m} + 2s - i(1-2s)qQ + 2(qQ + i(1-2s) + (qQ - is)\sin \nu)M\omega - 2(1 + \sin \nu)^2(M\omega)^2, \\ z_0 = 4iM\omega \sin \nu. \end{aligned} \quad (18)$$

For generic Q , the QNM calculation follows the procedure defined in (4), written in terms of the parameters (15) and (16) as

$$\tau_V(\vec{\theta}_{\text{non-ext}}; \sigma, \eta; z_0) = 0, \quad z_0 \frac{d}{dt} \log \tau_V(\vec{\theta}_{\text{non-ext}, -}; \sigma - 1, \eta; z_0) - \frac{\theta_-(\theta_+ - 1)}{2} = z_0 c_{z_0}, \quad (19)$$

with $\vec{\theta}_{\text{non-ext}} = \{\theta_-, \theta_+, \theta_*\}$, $\vec{\theta}_{\text{non-ext}} = \{\theta_-, \theta_+ - 1, \theta_* + 1\}$, the modulus and the accessory parameter given by (5). To distinguish from the extremal parameters we will introduce later, we have included the subscript non-ext. For the actual numerical analysis, it is more convenient to work directly with the system (19), rather than using the analysis at the end of Section (II).

A. Numerical Results for $\ell > |s|$

We are now ready to employ the technique described in the previous sections to determine the fundamental modes for spin-0 and spin- $\frac{1}{2}$ perturbations of the non-extremal RN black hole. The initial analysis is concentrated on the case $\ell > |s|$, which means $\ell = 1, 2, 3, \dots$ for the scalar case and $\ell = 3/2, 5/2, \dots$ for the spinorial case. As explained in [29], the potential terms for spin-1/2 produce the same QNMs spectrum for both values $s = \pm 1/2$ and there is no loss of generality in considering only the $s = -1/2$ case. Additionally, since the RN black hole is symmetric with respect to transformations $q \rightarrow -q$ and $\omega \rightarrow -\omega^*$, we consider only positive q and, consequently, $\Re(M\omega) > 0$.

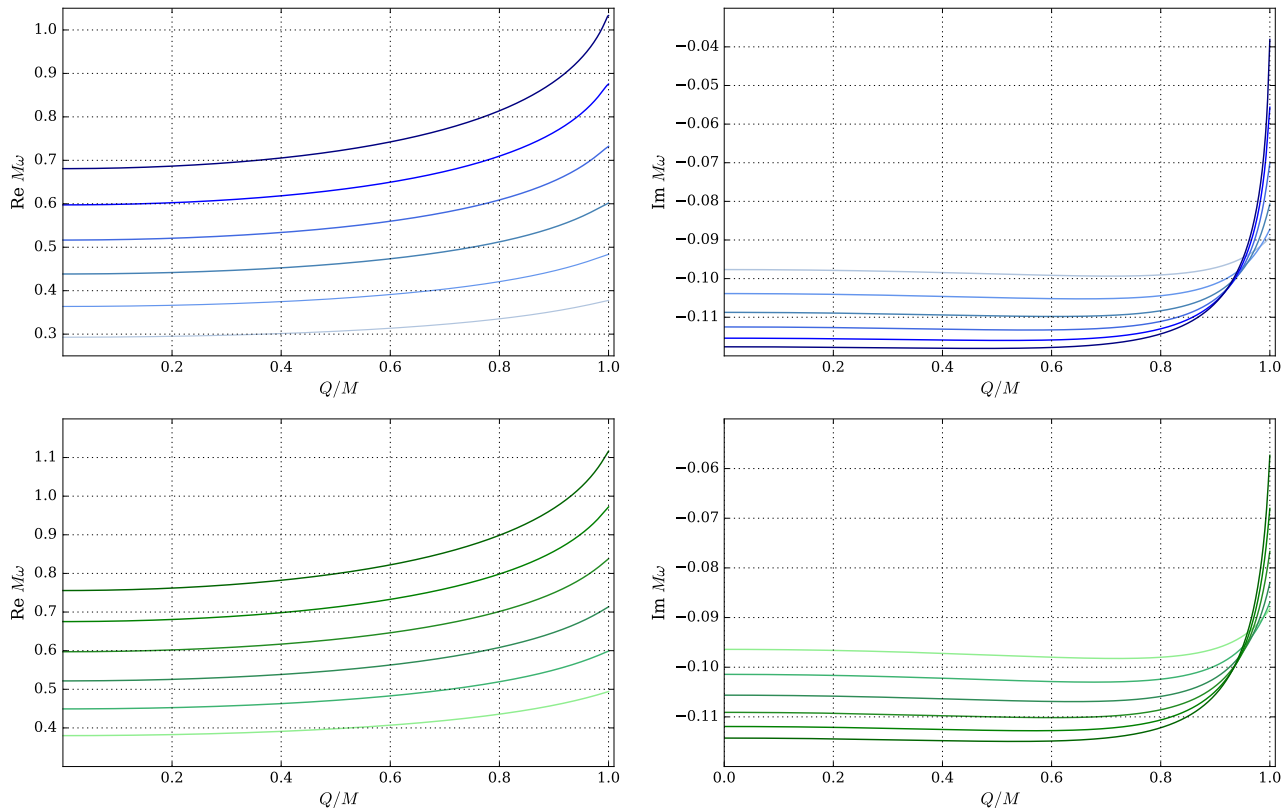


FIG. 1. Fundamental modes calculated for scalar and spinor perturbations in non-extremal RN black hole. Results for $s = 0, \ell = 1$ (top) and $s = -\frac{1}{2}, \ell = \frac{3}{2}$ (bottom) as a function of Q/M for $qQ = 0.0$ (lightest), 0.2, 0.4, 0.6, 0.8 and 1.0 (darkest).

In Fig. (1), we show the QNMs frequencies for $s = 0, \ell = 1$ and $s = -\frac{1}{2}, \ell = \frac{3}{2}$ as a function of qQ . These values were obtained by directly solving (19), using a numeric implementation of (6) and (5) in Julia language, finding the roots of τ_V using a simple root-finding algorithm (Muller's method). The Fredholm determinant involved in the definition of τ_V was truncated at $N_f = 32$ Fourier components and (5) at $N_c = 64$ convergents. The method converges fastly due to Miwa's theorem [30], which asserts that τ_V only has isolated and simple zeros away from its critical values $t = 0, \infty$. However, the zero locus structure can become very intricate, particularly close to extremality, so when varying $\frac{Q}{M}$ we use the QNM value for a particular point as the guess for the following point. The implementation of the Painlevé transcendents τ_{VI}, τ_V and τ_{III} based on the Fredholm determinants is available at [31].

When solving the set of equations (19), we have verified that the fundamental modes for $qQ = 0, Q/M = 0$, in the cases $s = 0, \ell = 1, 2, 3, \dots$, and $s = -\frac{1}{2}, \ell = \frac{3}{2}, \frac{5}{2}, \frac{7}{2}, \dots$, are in agreement with the modes for Schwarzschild black hole calculated using the WKB approximation [32, 33] and CF method in the literature, see Table 1. In turn, in the case of the non-extremal RN black hole with $qQ \neq 0$ and $Q/M = 0.999$, we recovered the fundamental modes for $s = 0, \ell = 1, 2, 3$ and $s = -\frac{1}{2}, \ell = \frac{3}{2}, \frac{5}{2}, \frac{7}{2}$ calculated using the modified version of the continued fraction method and listed in [12]. Given that the CF method has convergence problems near the extremality, we have extended the analysis by solving the system (19) for $Q \rightarrow M$, as we can see in Fig. 1. By employing the procedure described above, we can consider values up to $Q/M = 1 - 10^{-11}$ in reasonable time and accuracy. One notes that the method infers a smooth extremal limit for these modes, a point we will return to below.

s	ℓ	${}_s\omega_\ell$ (τ_V function)	${}_s\omega_\ell$ (CF method)
0	1	$0.292936133267 - 0.097659988914i$	$0.292936133267 - 0.097659988913i$
0	2	$0.483643872211 - 0.096758775978i$	$0.483643872211 - 0.096758775978i$
0	3	$0.675366232537 - 0.096499627734i$	$0.675366232537 - 0.096499627734i$
$-\frac{1}{2}$	$\frac{3}{2}$	$0.380036764833 - 0.096405208085i$	$0.380036764833 - 0.096405208085i$
$-\frac{1}{2}$	$\frac{5}{2}$	$0.574093974298 - 0.096304784939i$	$0.574093974298 - 0.096304784939i$
$-\frac{1}{2}$	$\frac{7}{2}$	$0.767354592773 - 0.096269878994i$	$0.767354592773 - 0.096269878994i$

TABLE I. To the left, the fundamental modes for Schwarzschild black hole $q = Q = 0$ recovered with $\ell > |s|$. For comparison, we show to the right the values in the literature [5].

B. Numerical Results for $\ell = |s|$

We now focus our attention in the case $\ell = |s|$ and investigate the behavior of the fundamental modes as Q/M and qQ vary. In our analysis, we have obtained QNMs for Q going from 0 to M as a function of qQ and observed two different types of behavior in the limite $Q \rightarrow M$, as follows:

- I. For qQ below a spin-dependent critical value $qQ_c(s)$ modes calculated from (19) behave similarly to $\ell > |s|$, with finite limits for the real and imaginary parts of the QNMs frequencies as $Q \rightarrow M$. Following [11], we will call these “damping modes”.
- II. For qQ above the spin-dependent critical value $qQ_c(s)$, the frequency converges to q as $Q \rightarrow M$ ($\nu \rightarrow 0$). In this case, the imaginary part of the QNM frequency tends to zero, in a non-damping behavior. Also, the existence of a natural small parameter allows for the analytical treatment of these modes.

Before checking each case separately, let us illustrate in Fig. 2 the qualitative difference between cases I and II in the usual graphs where $M\omega$ is plotted against Q/M . For $s = \ell = 0$, we note the appearance of non-trivial behavior for $Q \rightarrow M$ as one increases qQ . In this regime, the parametrization using ν (17) is more adequate, so we will switch to it. Also, one can appreciate the difficulty in studying these different behaviors using the usual CF method, given that it does not converge easily (if at all) as one approaches the extremal limit $\nu \rightarrow 0$.

The numerical analysis for these modes use the same procedure described above: we simply solve (19) for $\ell = |s|$. As a way of checking the procedure, we have recovered the fundamental mode for $qQ = 0$, $s = \ell = 0$, and $Q/M = 0$ obtained for scalar perturbation in the Schwarzschild black hole and listed in the literature. Also the fundamental mode for Dirac perturbation in this background was also retrieved and compared with our implementation of the CF method. This frequency was obtained in [32], using the WKB approximation which does not permit accurate comparisons. These values are presented in Table II. We have also checked our results for $qQ \neq 0$ and $Q/M \lesssim 0.999$ against [12] and found excellent agreement.

As one can observe from Fig. 2, the extremal limit $\nu \rightarrow 0$ of these modes shows non-trivial structure depending on the value of the coupling qQ . Let us now consider this limit in more detail.

s	ℓ	${}_s\omega_\ell$ (τ_V function)	${}_s\omega_\ell$ (CF method)
0	0	$0.110454939080 - 0.104895717087i$	$0.110454939080 - 0.104895717087i$
$-\frac{1}{2}$	$\frac{1}{2}$	$0.182962870255 - 0.096982392762i$	$0.182962870255 - 0.096982392762i$

TABLE II. Comparison of the fundamental QNMs frequencies for Schwarzschild $q = Q = 0$ black hole in the case $\ell = |s|$.

Non-damping modes for $\nu \rightarrow 0$

As the black hole approaches extremality, and qQ is large enough, the fundamental QNMs frequencies approach the purely real value $M\omega \rightarrow qQ$. Following [11], we will call these modes non-damping. Using the isomonodromic method, we can solve (19) numerically and study the behavior of the spin-0 and spin- $\frac{1}{2}$ modes as $\nu \rightarrow 0$. The result is displayed in Fig. 3, which can be understood as a zoomed in version of Fig. 2 at the near-extremal region. One notes a drastic bifurcation at a critical value $qQ_c(s)$, above which the modes become non-damping. We note that the extremal values for $qQ < qQ_c$ also have a distinct “almost constant” behavior for $\nu \rightarrow 0$ in contrast with the $\ell > |s|$ case.

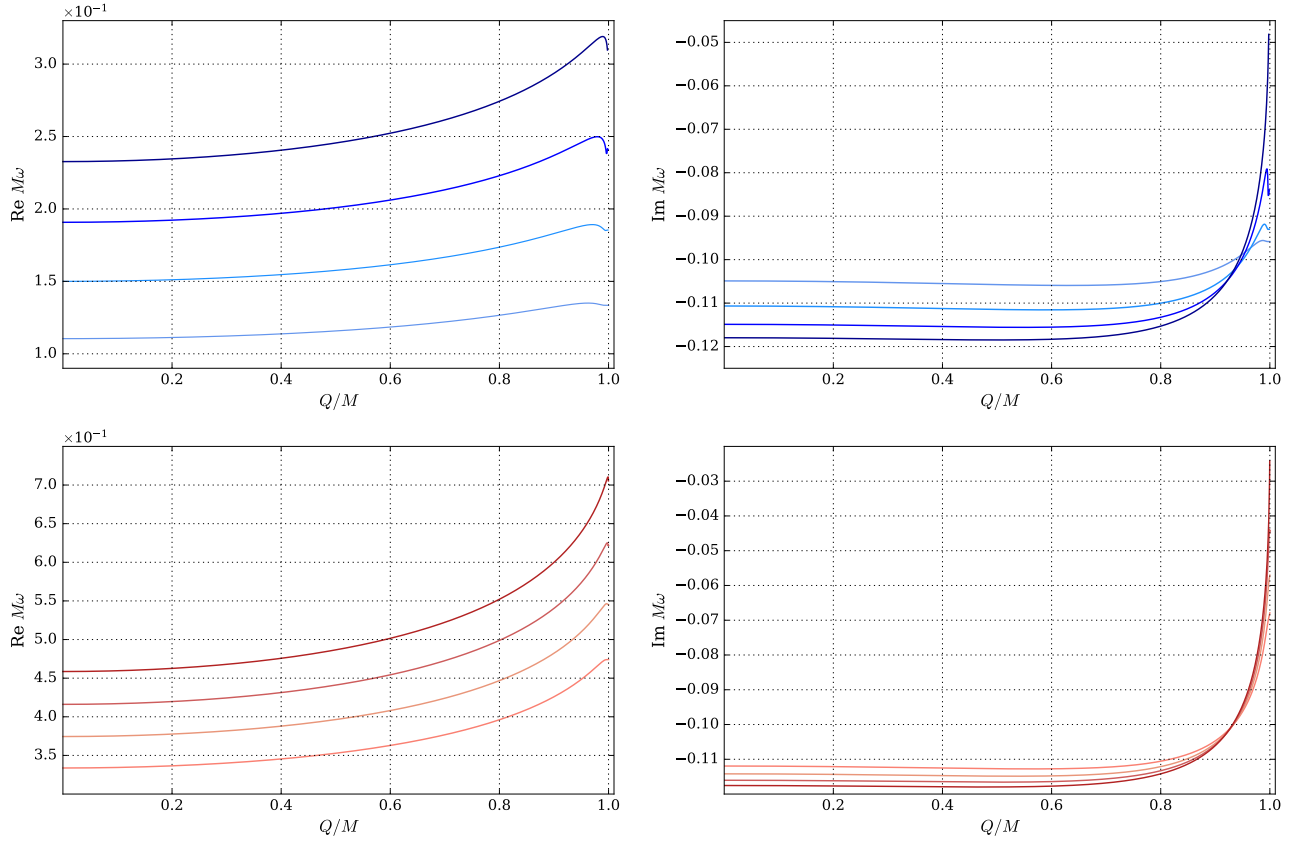


FIG. 2. Fundamental modes for $s = 0, l = 0$ (top) and $s = \frac{1}{2}, l = \frac{1}{2}$ (bottom) with qQ varying from 0 (lightest) to 0.3 (darkest) with 0.1 of increment.

In Fig. 4 we zoom into the transition for $s = 0$ and $s = -\frac{1}{2}$. A more careful numerical analysis yields critical values:

$$qQ_c(s = 0) \simeq 0.216228, \quad \text{and} \quad qQ_c(s = -1/2) \simeq 0.642745, \quad (20)$$

with the split at $\nu = \nu_c \simeq 0.078547$ for $s = 0$ and $\nu_c \simeq 0.027797$ for $s = -1/2$, corresponding to $Q/M \simeq 0.996917$ and $Q/M \simeq 0.999614$, respectively.

The non-damping modes also have the property that the associated single monodromy parameters θ_{\pm} in (17) have finite limits as $\nu \rightarrow 0$. Given that the isomonodromic expansion parameter z_0 is proportional to $\sin \nu$, it is also small in this limit and one can actually solve the equations (19) approximately by considering the first terms of the expansions involved. For the calculation of the QNMs frequencies, one can tackle the expansions for c_0 in (5) and χ_V in (13) in terms of ν directly. We follow the strategy of [21] and write the schematic expansion for the frequency and the composite monodromy parameter σ as

$$M\omega = qQ + \beta_1\nu + \beta_2\nu^2 + \dots, \quad \sigma = 1 + \alpha_0 + \alpha_1\nu + \alpha_2\nu^2 + \dots, \quad (21)$$

where the coefficients β_i and α_i may encode non-analytic corrections in ν , defining $M\omega$ and σ as formal transseries in ν and $\log \nu$. The values for α_i and β_i can be found recursively from the expansions (5) and (13). For instance, substitution of σ into (5) yields

$$\sigma = 1 + \alpha_0 + \frac{16qQ(2q^2Q^2 - s(3 + 4s) - 6_s\lambda_\ell)}{\alpha_0(\alpha_0^2 - 1)}\beta_1\nu + \dots, \quad (22)$$

where

$${}_s\lambda_\ell = (s - \ell)(s + \ell + 1), \quad \alpha_0 = \sqrt{(1 + 2\ell)^2 - 4q^2Q^2}. \quad (23)$$

With the value of σ at hand, we can substitute in (9) and find an equation for β_1 . We note that χ_V in the right-hand side of that equation is analytic in t_0 and thus can be written as expansion in ν . The non-analytic terms like $\log \nu$

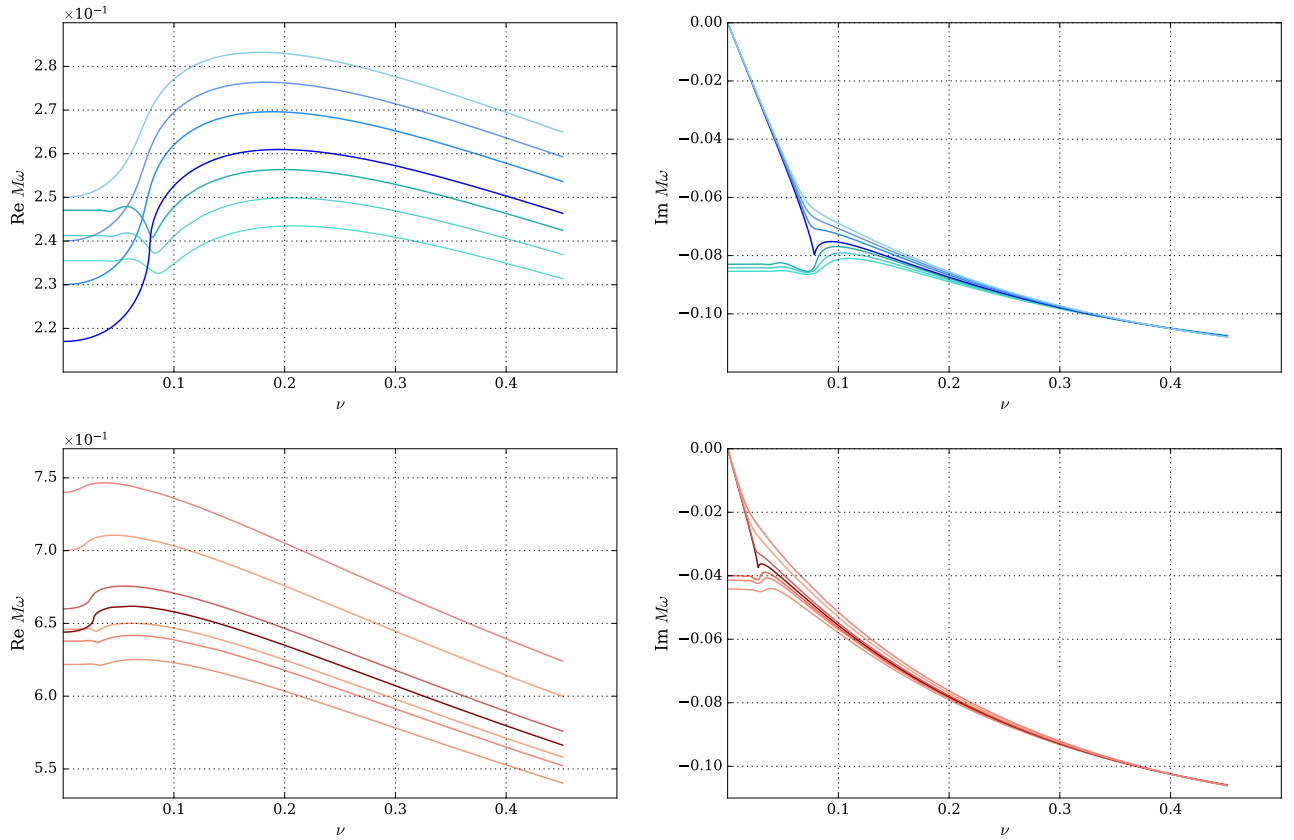


FIG. 3. Damping and non-damping modes for $s = 0, l = 0$ (top) and $s = -\frac{1}{2}, \ell = \frac{3}{2}$ (bottom) in near-extremal RN black hole. The dark color line identifies the critical values $qQ_c \approx 0.216$ ($s = 0, \ell = 0$) and $qQ_c \approx 0.643$ ($s = -\frac{1}{2}, \ell = \frac{1}{2}$).

arise from the expansion of the gamma functions in Θ_V (10). By considering the lowest-order contribution in ν , we find, after some algebra,

$$e^{-\frac{i\pi}{2}\alpha_0} \frac{\Gamma(1 - \alpha_0)^2 \Gamma(\frac{1}{2}(1 + \alpha_0) - i\beta_1) \Gamma(\frac{1}{2}(1 + \alpha_0) - iqQ - s) \Gamma(\frac{1}{2}(1 + \alpha_0) - iqQ + s)}{\Gamma(1 + \alpha_0)^2 \Gamma(\frac{1}{2}(1 - \alpha_0) - i\beta_1) \Gamma(\frac{1}{2}(1 - \alpha_0) - iqQ - s) \Gamma(\frac{1}{2}(1 - \alpha_0) - iqQ + s)} (4\nu qQ)^{\alpha_0} = 1 + \mathcal{O}(\nu, \nu \log \nu). \quad (24)$$

Assuming α_0 real and positive, the small ν regime of (24) simplifies considerably. The ν^{α_0} term becomes parametrically small, and the equation can be solved provided the argument of one of the gamma functions becomes very small, near its pole at vanishing argument. At any rate, this is the behavior we expect from the numerical analysis above the critical value $qQ_c < qQ \leq 1$. We therefore find that the first correction to the non-damping frequency is

$$\beta_1 = -\frac{1}{2}i(\alpha_0 + 1) + i \frac{(-i)^{\alpha_0} \Gamma(1 - \alpha_0)^2 \Gamma(\frac{1}{2}(\alpha_0 + 1) - iqQ + s) \Gamma(\frac{1}{2}(\alpha_0 + 1) - iqQ - s)}{\Gamma(-\alpha_0) \Gamma(1 + \alpha_0)^2 \Gamma(-s - \frac{1}{2}(\alpha_0 + 1) - iqQ) \Gamma(s - \frac{1}{2}(\alpha_0 + 1) - iqQ)} (4\nu qQ)^{\alpha_0} + \dots \quad (25)$$

again we note that the second term becomes irrelevant for small ν . Dropping this term and summarizing the result, we find the frequency to be

$$M\omega \simeq qQ - \frac{1}{2}i(\alpha_0 + 1)\nu = qQ - \frac{i}{2}(1 + \sqrt{(1 + 2\ell)^2 - 4q^2Q^2})\nu. \quad (26)$$

These modes, illustrated in Fig. 4, are the non-damping $qQ > qQ_c$ QNMs' frequencies with imaginary parts that vanish linearly with ν as $\nu \rightarrow 0$. For α_0 real, the near-extremal behavior of the real part of ω is quadratic, which again corroborates the findings of last Section. Similar remarks about the non-damping modes have been made by [34] using the CF method, albeit with a slightly different expression for α_0 .

From (26) one can also study the regime $qQ \gg \ell$, which is of interest to field propagation if not for perturbations of the background. Now the linear correction appears both to the real and imaginary parts of the frequency, and

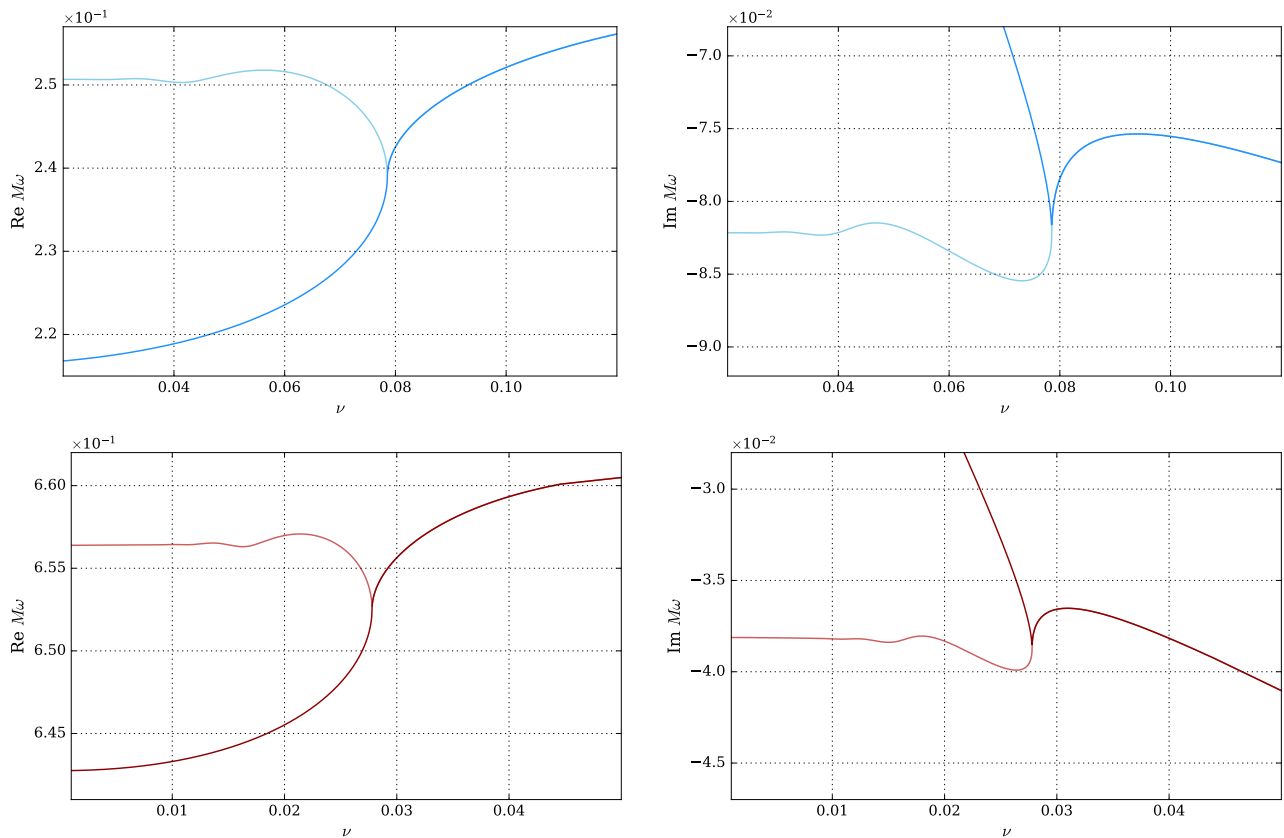


FIG. 4. Non-damping transitions for $\ell = |s|$ scalar (top) and spinor (bottom) modes for the RN black hole. The modes represented with darker color have coupling slightly above the critical value, whereas the lighter color are slightly below. Even with qQ differing only in the sixth decimal plane, they display radically different extremal limits in the region $\nu \leq \nu_c$.

expanding (26) in this regime yields

$$\omega \approx \frac{qQ}{M} + 2\pi qQ T_{BH} - \frac{i}{2}(2\pi)T_{BH} \quad (27)$$

in terms of the black-hole temperature $T_{BH} = T_+ \approx \frac{\nu}{2\pi M}$. A slightly different version of this result was presented in [35] using the WKB method.

We close by remarking that, despite the analysis pointing out that the non-damping modes are still perturbatively stable as $Q \rightarrow M$, the imaginary part becomes arbitrarily small, so one still has to consider a non-linear analysis to answer questions about the stability of the RN background. We hope to return to this issue in future work.

IV. CONFLUENT LIMIT AND EXTREMAL RN BLACK HOLE

For the modes with $\ell > |s|$ and $\ell = |s|$ with $qQ < qQ_c$, the QNM frequencies approach the extremal limit still keeping a finite imaginary part. In such cases, the extremal limit coincides with the confluent limit of the (3), written in terms of the parameters (15) as

$$\Lambda = \frac{1}{2}(\theta_t + \theta_0), \quad \theta_0 = \theta_t - \theta_0, \quad u_0 = \Lambda t_0, \quad \Lambda \rightarrow \infty, \quad (28)$$

leading to the double-confluent Heun equation

$$\frac{d^2 y}{du^2} + \left[\frac{2 - \theta_0}{u} - \frac{u_0}{u^2} \right] \frac{dy}{du} - \left[\frac{1}{4} + \frac{\theta_*}{2u} + \frac{u_0 c_{u_0} - u_0/2}{u^2} \right] y(u) = 0, \quad (29)$$

with two irregular singularities of Poincaré rank 1 at $z = 0$ and $z = \infty$ [36].

As seen in [21], the RH map for the double-confluent Heun equation can be cast in terms of the Third Painlevé transcendent. The confluent limit (28) of τ_V yielding its τ function, and (4) is replaced by

$$\tau_{III}(\vec{\theta}; \sigma, \eta; u_0) = 0, \quad z_0 \frac{d}{dt} \log \tau_{III}(\vec{\theta}_-; \sigma - 1, \eta; u_0) - \frac{(\theta_o - 1)^2}{2} = u_0 c_{u_0}. \quad (30)$$

Generic expressions for τ_{III} , listed in (A8), were also given in [18, 21]. We quote the first terms (A8)

$$\begin{aligned} \tau_{III}(\theta_*, \theta_o; \sigma, \eta; u) &= C_{III}(\vec{\theta}, \sigma) u^{\frac{1}{4}\sigma^2 - \frac{1}{8}\theta_o^2} e^{\frac{1}{2}u} \\ &\times \left(1 - \frac{\sigma - \theta_o \theta_*}{2\sigma^2} u - \frac{(\sigma + \theta_o)(\sigma + \theta_*)}{4\sigma^2(\sigma - 1)^2} \kappa_{III}^{-1} u^{1-\sigma} - \frac{(\sigma - \theta_o)(\sigma - \theta_*)}{4\sigma^2(\sigma + 1)^2} \kappa_{III} z^{1+\sigma} + \mathcal{O}(u^2, u^{2\pm 2\sigma}) \right) \end{aligned} \quad (31)$$

where

$$\kappa_{III} = e^{i\pi\eta} \Pi_{III} = e^{i\pi\eta} u^\sigma \frac{\Gamma(1 - \sigma)^2 \Gamma(1 + \frac{1}{2}(\theta_* + \sigma)) \Gamma(1 + \frac{1}{2}(\theta_o + \sigma))}{\Gamma(1 + \sigma)^2 \Gamma(1 + \frac{1}{2}(\theta_* - \sigma)) \Gamma(1 + \frac{1}{2}(\theta_o - \sigma))}. \quad (32)$$

We list in the Appendix expressions for τ_{III} in terms of Fredholm determinants, which we used in our numerical analysis. The confluent limit of (5) can also be taken

$$\begin{aligned} u_0 c_{u_0} &= \frac{(\sigma - 1)^2 - (\theta_o - 1)^2}{4} + \frac{\theta_o \theta_*}{4} \left(\frac{1}{\sigma - 2} - \frac{1}{\sigma} \right) u_0 \\ &\quad - \left[\frac{\theta_o^2 \theta_*^2}{16} \left(\frac{1}{(\sigma - 2)^3} - \frac{1}{2\sigma^3} \right) - \frac{\theta_o^2 + \theta_*^2 - \theta_o^2 \theta_*^2}{8\sigma(\sigma - 2)} - \frac{(\theta_o^2 - 1)(\theta_*^2 - 1)}{8(\sigma + 1)(\sigma - 3)} \right] u_0^2 + \mathcal{O}(u_0^3). \end{aligned} \quad (33)$$

Finally, following the same steps of the Section (II), we can take the confluent limit (28) of the condition (8). We therefore have that the boundary conditions relating to the QNMs are written in terms of the monodromy parameters as

$$e^{i\pi\eta} = e^{-2\pi i\sigma} \frac{\sin \frac{\pi}{2}(\theta_* + \sigma) \sin \frac{\pi}{2}(\theta_o + \sigma)}{\sin \frac{\pi}{2}(\theta_* - \sigma) \sin \frac{\pi}{2}(\theta_o - \sigma)}. \quad (34)$$

One can now consider the confluent limit of the parameters (15) of the radial equation (2). The single monodromy parameters are

$$\theta_{\text{ext},o} = \theta_o = 2s + 2i(-qQ + 2Q\omega), \quad \theta_{\text{ext},*} = \theta_* = -2s + 2i(2Q\omega - qQ) \quad (35)$$

and accessory parameter and modulus are now obtained by considering (18) in the appropriate confluent limit (28)

$$z_{\text{ext}} c_{z_{\text{ext}}} = {}_s\lambda_{l,m} + 2s - i(1 - 2s)qQ + 2(qQ + i(1 - 2s))M\omega - 8(M\omega)^2, \quad z_{\text{ext}} = -4M\omega(M\omega - qQ). \quad (36)$$

Formally, the RH map (30) for the double-confluent Heun equation is written in terms of the extremal parameters (35)

$$\tau_{III}(\vec{\theta}_{\text{ext}}; \sigma, \eta; z_{\text{ext}}) = 0, \quad z_{\text{ext}} \frac{d}{dt} \log \tau_{III}(\vec{\theta}_{\text{ext},-}; \sigma - 1, \eta; z_{\text{ext}}) - \frac{(\theta_{\text{ext},o} - 1)^2}{2} = z_{\text{ext}} c_{z_{\text{ext}}}, \quad (37)$$

with $\vec{\theta}_{\text{ext}} = \{\theta_o, \theta_*\}$, $\vec{\theta}_{\text{ext},-} = \{\theta_o - 1, \theta_* - 1\}$ and η given in (34).

As in the non-extremal case, the resolution of the equations (37) can be done directly given an implementation of the τ_{III} function. In Fig. 5 we plot the fundamental spin-0 and spin- $\frac{1}{2}$ perturbations for the extremal RN black hole as a function of qQ , for the $\ell > |s|$ case. As expected, modes with higher values of ℓ tend to decay faster, and the difference increases with qQ .

In Tables (III) and (IV) we give further support that the extremal limit of the $\ell > |s|$ modes is actually smooth, by solving the non-extremal equations (19) at Q/M very close to 1 and the actual extremal value computed numerically from (37). The values for $qQ = 0$ in the scalar case show good accordance with [37], whereas the spinor case agrees with [12] for $qQ < 0.1$. Unlike the CF method used in these references, the RH map allows us to compute the QNMs frequencies for arbitrary values of qQ .

For $\ell = |s|$ the QNM frequencies will be divided into two different classes, listed in II. For the interaction parameter qQ smaller than the critical value given in (20), the behavior of the QNM is similar to the $\ell > |s|$ case in which there will be a non-zero damping factor in the extremal limit. The values for the frequencies at extremality can also be computed from the equations (37). For qQ above the critical value, however, the mode “decouples” from the double-confluent equations, and the frequency becomes non-damped with value qQ/M . The behavior is illustrated in Fig. 6. Because of the non-damping modes, the question of stability of the extremal RN black hole under scalar and spinorial perturbations can only be settled by considering higher order terms in the Maxwell-Einstein equations.

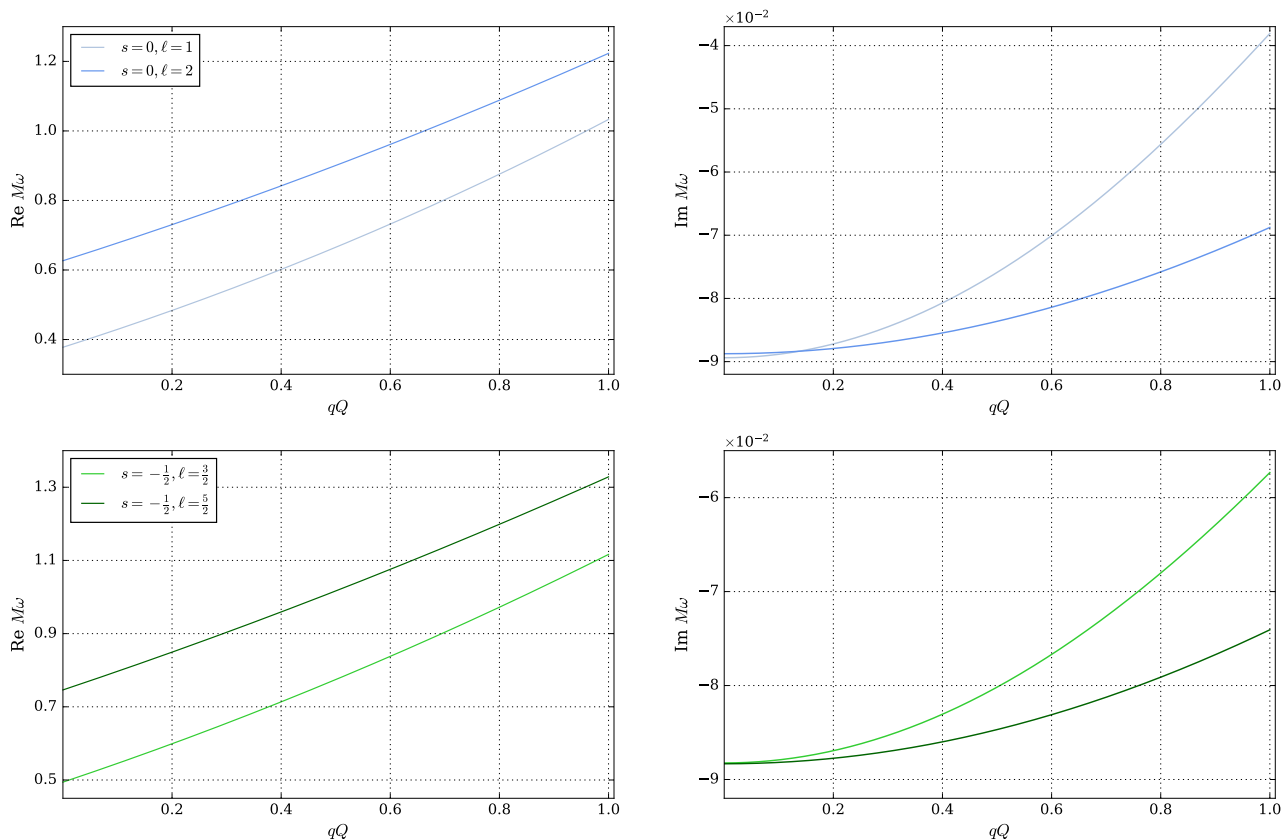


FIG. 5. Fundamental modes for $s = 0, l = 1, 2$ (top) and $s = -\frac{1}{2}, \ell = \frac{3}{2}, \frac{5}{2}$ (bottom) in extremal RN black hole ($Q = M$) as a function of qQ .

V. DISCUSSION

In this paper the authors used the isomonodromic method to study quasi-normal modes frequencies for scalar and spinorial perturbations of the Reissner-Nordström black hole. The map was derived by the authors in previous work [14], constructing monodromy parameters for generic solutions of the confluent Heun equation and making use of the expansions of the fifth and third Painlevé transcendents by [18, 19, 21], itself sparked by the deep relation between instanton counting and Liouville conformal blocks [38, 39]. Although we have made use of the “ $c = 1$ ” version of the relation – or rather, the Riemann-Hilbert problem formulation of the relation, there is growing interest in the semiclassical “Nekrasov-Shatashvili” version of the relation [20, 40], which also proposes to compute accessory parameters for Fuchsian differential equations, and their confluent limits, given monodromy data. For the practical purpose of solving boundary problems like finding QNM frequencies, expressions like (4) and (30) provide not only a formal solution to the system, but also a means of calculation which is unencumbered by the shortcomings of the usual CF and WKB methods [41]. In [42], the authors gave a comprehensive list of properties of the Kerr background like greybody factors, QNMs and Love numbers in terms of monodromy parameters.

For the RN black hole, the analysis is comparatively simpler, since the angular problem can be solved exactly in terms of spin-weighted spherical harmonics. We have found that the behavior of the QNMs parallels those found for Kerr in [21], along with the modes which decay even in the extremal limit, there are non-damping modes for $\ell = |s|$ whose relaxation time diverges with the inverse temperature as one approaches $Q = M$. These non-damping modes parallel the co-rotating QNMs in Kerr geometry, and we have found the transition to happen above a critical value for the interaction parameter (20). This parameter plays a role for RN similar to the angular momentum to Kerr, and, unlike m , it can be varied continuously. We have found the critical value qQ_c to be a bifurcation point in the sense that for small enough extremality parameter ν , the behavior of the QNMs changes abruptly as the interaction parameter crosses qQ_c . The actual mechanism for this transition certainly needs clarification, and we hope to return to this issue in the future. Here we have kept our analysis to scalar and spinor modes, but, given the wide scope of the RH map, we have every reason to expect that the method will work for higher spin perturbations as well.

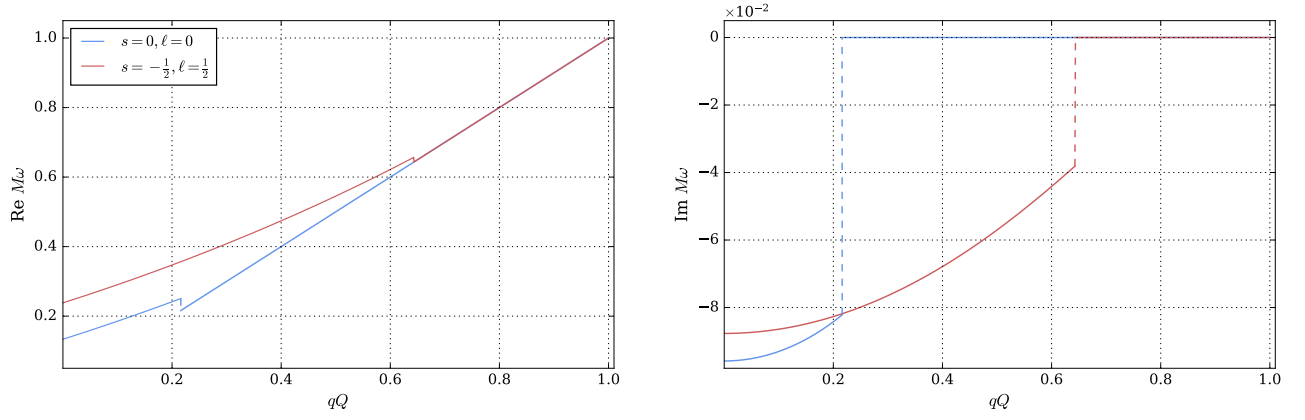


FIG. 6. QNMs for $\ell = |s|$ in the scalar (blue) and spinorial (red) cases. For the interaction parameter less than the critical value of (20), the values are calculable from the τ_{III} function. Above the critical value, the modes are non-damping and the imaginary values of the eigenfrequencies go abruptly to zero.

qQ	$\ell = 1$		$\ell = 2$	
	$Q/M = 0.999999$	$Q/M = 1$	$Q/M = 0.999999$	$Q/M = 1$
0.0	0.3776416 - 0.0893845i	0.3776418 - 0.0893843i	0.6265722 - 0.0887485i	0.6265727 - 0.0887483i
0.1	0.4291343 - 0.0888385i	0.4291346 - 0.0888382i	0.6775330 - 0.0885422i	0.6775336 - 0.0885419i
0.2	0.4836193 - 0.0872035i	0.4836196 - 0.0872031i	0.7304163 - 0.0879239i	0.7304170 - 0.0879236i
0.3	0.5411167 - 0.0844886i	0.5411172 - 0.0844882i	0.7852239 - 0.0868961i	0.7852248 - 0.0868957i
0.4	0.6016610 - 0.0807101i	0.6016616 - 0.0807095i	0.8419591 - 0.0854624i	0.8419601 - 0.0854620i
0.5	0.6653021 - 0.0758925i	0.6653028 - 0.0758917i	0.9006264 - 0.0836285i	0.9006276 - 0.0836280i
0.6	0.7321070 - 0.0700711i	0.7321078 - 0.0700701i	0.9612317 - 0.0814015i	0.9612330 - 0.0814008i
0.7	0.8021625 - 0.0632953i	0.8021634 - 0.0632939i	1.0237821 - 0.0787904i	1.0237836 - 0.0787896i
0.8	0.8755790 - 0.0556340i	0.8755799 - 0.0556320i	1.0882862 - 0.0758061i	1.0882879 - 0.0758052i
0.9	0.9524949 - 0.0471845i	0.9524959 - 0.0471819i	1.1547541 - 0.0724620i	1.1547561 - 0.0724608i
1.0	1.0330846 - 0.0380869i	1.0330854 - 0.0380833i	1.2231973 - 0.0687733i	1.2231995 - 0.0687720i

TABLE III. A comparison between the fundamental modes for scalar $s = 0$ perturbations of the RN black hole computed from (19) with Q/M very close to 1, and those computed in the extremal case using (37) for various values of the interaction parameter qQ .

We hope that the method developed in the aforementioned papers and applied here proves to be an invaluable tool in the calculation of black hole perturbations, both in the asymptotically flat case and otherwise [43–45]. With the comparatively nice properties of the isomonodromic τ -functions involved, one can perhaps utilize it to even shed light on the full, nonlinear, stability issues [46].

VI. ACKNOWLEDGEMENTS

The authors thank A. Grassi, A. Tanzini and S. Hod for comments and suggestions. JPC acknowledges partial support from CNPq.

Appendix A: τ_V and τ_{III} function and Quantization condition

The Fredholm determinant expression for τ_V is given by

$$\tau_V(\vec{\theta}; \sigma, \eta; t) = t^{\frac{1}{4}(\sigma^2 - \theta_0^2 - \theta_i^2)} e^{\frac{1}{2}\theta_i t} \det(\mathbb{1} - A \kappa_V^{\frac{1}{2}\sigma_3} t^{\frac{1}{2}\sigma\sigma_3} D_c(t) \kappa_V^{-\frac{1}{2}\sigma_3} t^{-\frac{1}{2}\sigma\sigma_3}) \quad (\text{A1})$$

qQ	$\ell = 3/2$		$\ell = 5/2$	
	$Q/M = 0.999999$	$Q/M = 1$	$Q/M = 0.999999$	$Q/M = 1$
0.0	0.4941127 - 0.0882400i	0.4941131 - 0.0882398i	0.7460834 - 0.0883267i	0.7460841 - 0.0883265i
0.1	0.5453239 - 0.0879134i	0.5453244 - 0.0879132i	0.7969051 - 0.0881804i	0.7969059 - 0.0881802i
0.2	0.5989590 - 0.0869355i	0.5989596 - 0.0869352i	0.8493706 - 0.0877419i	0.8493715 - 0.0877416i
0.3	0.6550227 - 0.0853120i	0.6550234 - 0.0853119i	0.9034806 - 0.0870124i	0.9034816 - 0.0870120i
0.4	0.7135223 - 0.0830539i	0.7135231 - 0.0830534i	0.9592359 - 0.0859942i	0.9592370 - 0.0859938i
0.5	0.7744686 - 0.0801747i	0.7744696 - 0.0801740i	1.0166382 - 0.0846905i	1.0166394 - 0.0846901i
0.6	0.8378753 - 0.0766939i	0.8378764 - 0.0766930i	1.0756891 - 0.0831055i	1.0756906 - 0.0831049i
0.7	0.9037594 - 0.0726358i	0.9037607 - 0.0726347i	1.1363911 - 0.0812441i	1.1363927 - 0.0812434i
0.8	0.9721413 - 0.0680306i	0.9721429 - 0.0680293i	1.1987468 - 0.0791125i	1.1987486 - 0.0791117i
0.9	1.0430450 - 0.0629152i	1.0430468 - 0.0629135i	1.2627593 - 0.0767178i	1.2627613 - 0.0767169i
1.0	1.1164980 - 0.0573342i	1.1165001 - 0.0573321i	1.3284321 - 0.0740684i	1.3284344 - 0.0740674i

TABLE IV. The comparison between fundamental modes for spinorial $s = -1/2$ perturbations of the RN black hole obtained from near-extremal (19) and extremal (37) as a function of qQ .

where A and D_c are operators acting on pair of analytic functions defined on a circle \mathcal{C} of radius $R < 1$,

$$(Ag)(z) = \oint_{\mathcal{C}} \frac{dz'}{2\pi i} A(z, z')g(z'), \quad (D_c g)(z) = \oint_{\mathcal{C}} \frac{dz'}{2\pi i} D_c(z, z')g(z'), \quad g(z') = \begin{pmatrix} f_+(z) \\ f_-(z) \end{pmatrix} \quad (\text{A2})$$

with kernels given explicitly for $|t| < R$, by

$$A(z, z') = \frac{\Psi^{-1}(\sigma, \theta_t, \theta_0; z')\Psi(\sigma, \theta_t, \theta_0; z) - \mathbb{1}}{z - z'}, \quad (\text{A3})$$

$$D_c(z, z') = \frac{\mathbb{1} - \Psi_c^{-1}(-\sigma, \theta_*, t/z')\Psi_c(-\sigma, \theta_*, t/z)}{z - z'},$$

where the parametres Ψ and Ψ_c are matrices whose entries are given by

$$\Psi(\sigma, \theta_t, \theta_0; z) = \begin{pmatrix} \phi(\sigma, \theta_t, \theta_0; z) & \chi(-\sigma, \theta_t, \theta_0; z) \\ \chi(\sigma, \theta_t, \theta_0; z) & \phi(-\sigma, \theta_t, \theta_0; z) \end{pmatrix}, \quad (\text{A4})$$

with ϕ and χ in terms of Gauss' hypergeometric series

$$\phi(\sigma, \theta_t, \theta_0; z) = {}_2F_1\left(\frac{1}{2}(\sigma - \theta_t + \theta_0), \frac{1}{2}(\sigma - \theta_t - \theta_0); \sigma; z\right)$$

$$\chi(\sigma, \theta_t, \theta_0; z) = \frac{\theta_0^2 - (\sigma - \theta_t)^2}{4\sigma(1 + \sigma)} {}_2F_1\left(1 + \frac{1}{2}(\sigma - \theta_t + \theta_0), 1 + \frac{1}{2}(\sigma - \theta_t - \theta_0); 2 + \sigma; z\right) \quad (\text{A5})$$

and

$$\Psi_c(-\sigma, \theta_*, t/z) = \begin{pmatrix} \phi_c(-\sigma, \theta_*, t/z) & \chi_c(-\sigma, \theta_*, t/z) \\ \chi_c(\sigma, \theta_*, t/z) & \phi_c(\sigma, \theta_*, t/z) \end{pmatrix},$$

$$\phi_c(\pm\sigma, \theta_*, t/z) = {}_1F_1\left(\frac{-\theta_* \pm \sigma}{2}; \pm\sigma; -t/z\right), \quad (\text{A6})$$

$$\chi_c(\pm\sigma, \theta_*, t/z) = \pm \frac{-\theta_* \pm \sigma}{2\sigma(1 \pm \sigma)} \frac{t}{z} {}_1F_1\left(1 + \frac{-\theta_* \pm \sigma}{2}, 2 \pm \sigma; -t/z\right), \quad (\text{A7})$$

where ${}_1F_1$ the confluent (Kummer's) hypergeometric series. Finally, the κ_V parameter is defined in terms of monodromy data by (7).

The version of the third Painlevé transcendent τ -function used here was derived in [21]. The expression is formally similar to (A1)

$$\tau_{III}(\theta_*, \theta_0; \sigma, \eta; u) = u^{\frac{1}{4}\sigma^2 - \frac{1}{8}\theta_0^2} e^{\frac{1}{2}u} \det(\mathbb{1} - A_c \kappa_{III}^{\frac{1}{2}\sigma_3} u^{\frac{1}{2}\sigma\sigma_3} D_c(u) \kappa_{III}^{-\frac{1}{2}\sigma_3} u^{-\frac{1}{2}\sigma\sigma_3}). \quad (\text{A8})$$

where D_c is as above and the kernel of A_c is now also given by confluent hypergeometric functions

$$A_c(z, z') = \frac{\Psi_c^{-1}(\sigma, \theta_0; z') \Psi_c(\sigma, \theta_0; z) - \mathbb{1}}{z - z'}, \quad (\text{A9})$$

with Ψ_c as in (A) and κ_{III} given in terms of monodromy data by (32).

If one starts from (A1) and (A8), by expanding the determinants to first order in t and u one recovers the first terms in the expansions given by (6) and (31), respectively. In order to make use of these expressions numerically, we wrote the matrix elements of the operators in a Fourier basis – on the circle \mathcal{C} – effectively reducing the Fredholm operator to a finite matrix after truncating the basis to order N_f . The interested reader can find the details in [21] or in [31], where an implementation in Julia is available.

1. Quantization Condition

To derive the quantization condition one uses the following set of local solutions of (3) near $z = t_0$ and $z = \infty$,

$$y_{t_0,+}(z) = (z - t_0)^{\theta_t}(1 + \mathcal{O}(z - t_0)), \quad y_{t_0,-}(z) = (z - t_0)^0(1 + \mathcal{O}(z - t_0)), \quad (\text{A10})$$

$$y_{\infty,+}(z) = e^z z^{-\theta_\star/2}(1 + \mathcal{O}(1/z)), \quad y_{\infty,-}(z) = e^{-z} z^{\theta_\star/2}(1 + \mathcal{O}(1/z)), \quad (\text{A11})$$

where $y_{t,\pm}$ form a basis of solutions near $z = t_0$, while $y_{\infty,\pm}$ represent a basis near of $z = \infty$.

After some algebraic manipulation of the monodromy matrices, the connection matrix C_t between these local solutions are written in the following form

$$\begin{pmatrix} \rho_\infty y_{\infty,+}(z) \\ \tilde{\rho}_\infty y_{\infty,-}(z) \end{pmatrix} = C_t \begin{pmatrix} \rho_{t_0} y_{t_0,+}(z) \\ \tilde{\rho}_{t_0} y_{t_0,-}(z) \end{pmatrix} = \begin{pmatrix} e^{-\frac{i\pi}{2}\eta} \zeta'_{t_0} - e^{\frac{i\pi}{2}\eta} \zeta_{t_0} & -e^{-\frac{i\pi}{2}\eta} \zeta_\infty \zeta'_{t_0} + e^{\frac{i\pi}{2}\eta} \zeta'_\infty \zeta_{t_0} \\ e^{-\frac{i\pi}{2}\eta} - e^{\frac{i\pi}{2}\eta} & -e^{-\frac{i\pi}{2}\eta} \zeta_\infty + e^{\frac{i\pi}{2}\eta} \zeta'_\infty \end{pmatrix} \begin{pmatrix} \rho_{t_0} y_{t_0,+}(z) \\ \tilde{\rho}_{t_0} y_{t_0,-}(z) \end{pmatrix} \quad (\text{A12})$$

with

$$\begin{aligned} \zeta_\infty &= e^{\frac{i\pi}{2}\sigma} \sin \frac{\pi}{2}(\theta_\star + \sigma), & \zeta'_\infty &= e^{-\frac{i\pi}{2}\sigma} \sin \frac{\pi}{2}(\theta_\star - \sigma), \\ \zeta_{t_0} &= \sin \frac{\pi}{2}(\theta_t + \theta_0 - \sigma) \sin \frac{\pi}{2}(\theta_t - \theta_0 - \sigma), & \zeta'_{t_0} &= \sin \frac{\pi}{2}(\theta_t + \theta_0 + \sigma) \sin \frac{\pi}{2}(\theta_t - \theta_0 + \sigma), \end{aligned} \quad (\text{A13})$$

and $\rho_t, \tilde{\rho}_t, \rho_\infty, \tilde{\rho}_\infty$ are (in principle arbitrary) normalization constants. In the calculation of quasi-normal modes, we should constraint C_t to be lower triangular. We then have an expression for η

$$e^{i\pi\eta} = \frac{\zeta_\infty \zeta'_{t_0}}{\zeta'_{t_0} \zeta_\infty}, \quad (\text{A14})$$

which, when written in terms of the monodromy parameters, gives (8).

-
- [1] R. M. Wald, *General Relativity*. The University of Chicago Press, 1984.
- [2] S. A. Teukolsky, *Perturbations of a rotating black hole. I. Fundamental equations for gravitational, electromagnetic, and neutrino-field perturbations*, *The Astrophysical Journal* **185** (1973) 635–648.
- [3] K. D. Kokkotas and B. G. Schmidt, *Quasi-normal modes of stars and black holes*, *LivingRev.Rel.* **2:2,1999** (LivingRev.Rel.2:2,1999) [[gr-qc/9909058](#)].
- [4] J. N. Goldberg, A. J. Macfarlane, E. T. Newman, F. Rohrlich, and E. C. G. Sudarshan, *Spin-s spherical harmonics and δ* , *Journal of Mathematical Physics* **8** (1967), no. 11 2155–2161.
- [5] E. Berti, V. Cardoso, and M. Casals, *Eigenvalues and eigenfunctions of spin-weighted spheroidal harmonics in four and higher dimensions*, *Phys.Rev.* **D73** (2006) 024013, [[gr-qc/0511111](#)].
- [6] K. D. Kokkotas and B. F. Schutz, *Black Hole Normal Modes: A WKB Approach. 3. The Reissner-Nordstrom Black Hole*, *Phys. Rev. D* **37** (1988) 3378–3387.
- [7] E. W. Leaver, *Quasinormal modes of reissner-nordström black holes*, *Phys. Rev. D* **41** (May, 1990) 2986–2997.
- [8] E. Leaver, *An Analytic representation for the quasi normal modes of Kerr black holes*, *Proc.Roy.Soc.Lond.* **A402** (1985) 285–298.
- [9] H. Onozawa, T. Mishima, T. Okamura, and H. Ishihara, *Quasinormal modes of maximally charged black holes*, *Phys. Rev. D* **53** (1996) 7033–7040, [[gr-qc/9603021](#)].
- [10] Y.-J. Wu and Z. Zhao, *Dirac quasinormal modes in Reissner-Nordstrom spacetimes*, *Phys. Rev. D* **69** (2004) 084015.

- [11] M. Richartz and D. Giugno, *Quasinormal modes of charged fields around a Reissner-Nordström black hole*, *Phys. Rev. D* **90** (2014), no. 12 124011, [arXiv:1409.7440].
- [12] M. Richartz, *Quasinormal modes of extremal black holes*, *Phys. Rev. D* **93** (2016), no. 6 064062, [arXiv:1509.04260].
- [13] B. Carneiro da Cunha and F. Novaes, *Kerr Scattering Coefficients via Isomonodromy*, *JHEP* **11** (2015) 144, [arXiv:1506.06588].
- [14] B. Carneiro da Cunha and J. P. Cavalcante, *Confluent conformal blocks and the Teukolsky master equation*, *Phys. Rev. D* **102** (2020), no. 105013 [arXiv:1906.10638].
- [15] L. Motl and A. Neitzke, *Asymptotic black hole quasinormal frequencies*, *Adv.Theor.Math.Phys.* **7** (2003) 307–330, [hep-th/0301173].
- [16] A. Neitzke, *Greybody factors at large imaginary frequencies*, hep-th/0304080.
- [17] A. Castro, J. M. Lapan, A. Maloney, and M. J. Rodriguez, *Black Hole Scattering from Monodromy*, *Class.Quant.Grav.* **30** (2013) 165005, [arXiv:1304.3781].
- [18] O. Gamayun, N. Iorgov, and O. Lisovyy, *How instanton combinatorics solves Painlevé VI, V and IIIs*, *J.Phys.* **A46** (Feb., 2013) 335203, [arXiv:1302.1832].
- [19] O. Lisovyy, H. Nagoya, and J. Roussillon, *Irregular conformal blocks and connection formulae for Painlevé V functions*, *J. Math. Phys.* **59** (2018), no. 9 091409, [arXiv:1806.08344].
- [20] M. Bershtein, P. Gavrylenko, and A. Grassi, *Quantum spectral problems and isomonodromic deformations*, arXiv:2105.00985.
- [21] B. Carneiro da Cunha and J. P. Cavalcante, *Teukolsky master equation and Painlevé transcendents: numerics and extremal limit*, arXiv:2105.08790.
- [22] K. Okamoto, *Studies on the Painlevé equations II. Fifth Painlevé equation P_V* , *Japanese journal of mathematics. New series* **13** (1987), no. 1 47–76.
- [23] M. Jimbo, T. Miwa, and A. K. Ueno, *Monodromy Preserving Deformation of Linear Ordinary Differential Equations With Rational Coefficients, I*, *Physica* **D2** (1981) 306–352.
- [24] M. Jimbo and T. Miwa, *Monodromy Preserving Deformation of Linear Ordinary Differential Equations with Rational Coefficients, II*, *Physica* **D2** (1981) 407–448.
- [25] M. Jimbo and T. Miwa, *Monodromy Preserving Deformation of Linear Ordinary Differential Equations with Rational Coefficients, III*, *Physica* **D4** (1981) 26–46.
- [26] O. Lisovyy and A. Naidiuk, *Accessory parameters in confluent Heun equations and classical irregular conformal blocks*, arXiv:2101.05715.
- [27] A. Litvinov, S. Lukyanov, N. Nekrasov, and A. Zamolodchikov, *Classical Conformal Blocks and Painleve VI*, arXiv:1309.4700.
- [28] M. Jimbo, *Monodromy Problem and the boundary condition for some Painlevé equations*, *Publ. Res. Inst. Math. Sci.* **18** (1982) 1137–1161.
- [29] J. Chang and Y. Shen, *Massive Charged Quasinormal Modes of a Reissner-Nordström Black Hole*, *International Journal of Theoretical Physics* **46** (2007) 1570–1583.
- [30] T. Miwa, *Painlevé property of monodromy preserving deformation equations and the analyticity of τ functions*, *Publications of the Research Institute for Mathematical Sciences* **17** (1981), no. 2 703–721.
- [31] <https://github.com/strings-ufpe/painleve>.
- [32] R. A. Konoplya, *Quasinormal modes of the Schwarzschild black hole and higher order WKB approach*, *J. Phys. Stud.* **8** (2004) 93–100.
- [33] H. T. Cho, *Dirac quasinormal modes in Schwarzschild black hole space-times*, *Phys. Rev. D* **68** (2003) 024003, [gr-qc/0303078].
- [34] M. Richartz, C. A. R. Herdeiro, and E. Berti, *Synchronous frequencies of extremal Kerr black holes: resonances, scattering and stability*, *Phys. Rev. D* **96** (2017), no. 4 044034, [arXiv:1706.01112].
- [35] S. Hod, *Quasinormal resonances of a charged scalar field in a charged Reissner-Nordstrom black-hole spacetime: A WKB analysis*, *Phys. Lett. B* **710** (2012) 349–351, [arXiv:1205.5087].
- [36] “NIST Digital Library of Mathematical Functions.” <http://dlmf.nist.gov/>, Release 1.1.2 of 2021-06-15. F. W. J. Olver, A. B. Olde Daalhuis, D. W. Lozier, B. I. Schneider, R. F. Boisvert, C. W. Clark, B. R. Miller, B. V. Saunders, H. S. Cohl, and M. A. McClain, eds.
- [37] H. Onozawa, T. Mishima, T. Okamura, and H. Ishihara, *Quasinormal modes of maximally charged black holes*, *Phys. Rev. D* **53** (Jun, 1996) 7033–7040.
- [38] L. F. Alday, D. Gaiotto, and Y. Tachikawa, *Liouville Correlation Functions from Four-dimensional Gauge Theories*, *Lett.Math.Phys.* **91** (2010) 167–197, [arXiv:0906.3219].
- [39] V. A. Alba, V. A. Fateev, A. V. Litvinov, and G. M. Tarnopolskiy, *On combinatorial expansion of the conformal blocks arising from AGT conjecture*, *Lett.Math.Phys.* **98** (2011) 33–64, [arXiv:1012.1312].
- [40] S. Jeong and N. Nekrasov, *Riemann-Hilbert correspondence and blown up surface defects*, arXiv:2007.03660.
- [41] G. Aminov, A. Grassi, and Y. Hatsuda, *Black Hole Quasinormal Modes and Seiberg-Witten Theory*, arXiv:2006.06111.
- [42] G. Bonelli, C. Iossa, D. P. Lichtig, and A. Tanzini, *Exact solution of Kerr black hole perturbations via CFT_2 and instanton counting*, arXiv:2105.04483.
- [43] F. Novaes, C. Marinho, M. Lencsés, and M. Casals, *Kerr-de Sitter Quasinormal Modes via Accessory Parameter Expansion*, arXiv:1811.11912.
- [44] J. Barragán Amado, B. Carneiro da Cunha, and E. Pallante, *Scalar quasinormal modes of Kerr-AdS5*, *Phys. Rev.* **D99** (2019), no. 10 105006, [arXiv:1812.08921].

- [45] J. Barragán-Amado, B. Carneiro da Cunha, and E. Pallante, *Vector perturbations of Kerr-AdS₅ and the Painlevé VI transcendent*, [arXiv:2002.06108](#).
- [46] S. R. Green, S. Hollands, and P. Zimmerman, *Teukolsky formalism for nonlinear Kerr perturbations*, *Class. Quant. Grav.* **37** (2020), no. 7 075001, [[arXiv:1908.09095](#)].